M&C 2001 Salt Lake City, Utah, USA, September 2001.

SINGLE RAY STREAMING BEHAVIOR FOR DISCONTINUOUS FINITE ELEMENT SPATIAL DISCRETIZATIONS

R. P. Smedley-Stevenson
AWE
Aldermaston, Reading, RG7 4PR, UK
rsmedley-stevenson@awe.co.uk

Keywords: DFEMs, ray propagation, slope limiters, mass lumping

ABSTRACT

This paper compares the results for streaming along a single ray direction from linear discontinuous finite element (DFEM) discretizations of the transport equation using both Galerkin and Petrov-Galerkin weight functions. The utility of a slope limiter to remove extrema from the transport solution is investigated as an alternative to mass lumping of the removal operator; the latter procedure introduces significant numerical diffusion and can destroy the fidelity of the solution. Results are presented for single ray propagation in slab geometry and two-dimensional (2D) planar geometry.

1. INTRODUCTION

An algorithm for solving the time-dependent thermal radiation transport equation using discontinuous finite elements (DFEMs) for the spatial variation and a discrete-ordinate like angular discretization has been developed by the author (Smedley-Stevenson, 2000 and Smedley-Stevenson, 2000[a]). The solution of the transport equation is required for unstructured meshes of quadrilaterals generated by Lagrangian and arbitrary Lagrange-Eulerian (ALE) hydrodynamics calculations for planar geometry in both two and three dimensions and also 2D axi-symmetric geometry.

This is coupled to a mass lumped continuous finite element (CFEM) solution of the time-dependent material energy equation by linearizing the thermal emission source term using the linearized multi-frequency grey method (Morel, 1996) for multi-group problems. The aim is to be able to perform high-fidelity coupled radiation hydrodynamics simulations by linking this radiation transport module to a shock physics code.

This computational algorithm will be validated against benchmark solutions of thermal radiation problems (see for example Su and Olson (1997)). Prior to commencing this validation effort it was decided to study the fidelity of single ray propagation with reference to the work of Mathews (1999). This raises serious issues concerned with the fidelity of DFEM spatial discretizations of the transport equation.

1.1 Ray propagation

In spatially discretizing the transport equation it is reasonable to ask how well can the discrete scheme model the transport of particles through the mesh. Do the particles propagate along straight-lines independent of the spatial mesh or do distortions present in the spatial grid unduly influence the flow. It is likely that the ray will be smeared in space as it propagates as any discretization scheme has a tendency to wash out singularities in the initial and/or boundary conditions and produce smooth solutions. This may lead to the generation of negative intensities on either side of the ray due to undershoots but these should be heavily damped so that they do not persist for more than a few cell widths on either side of the ray.

A related question is the accuracy of the attenuation of the ray due to the removal operator and also the smearing out of the wavefront shape over space (equivalent to a smearing over time). For this latter difficulty it is possible to draw an analogy with the problem of advecting concentration distributions for species moving through the computational domain in fluid dynamics simulations. The wealth of research in this related field can be exploited to provide methods for improving the fidelity of the solution of the transport equation, although to the author's knowledge the cross pollenation between these entirely separate disciplines has not been heavily exploited in the past.

This paper concentrates on the fidelity of the solution of the transport equation along a single ray direction for DFEM discretizations in vacuum and purely absorbing media, highlighting the relative advantages and disadvantages of Galerkin and Petrov-Galerkin weighting of the transport equation for single ray propagation. This is fundamental to establishing the accuracy of any algorithm used to solve the transport equation.

Potential improvements to the fidelity of the solution are considered. The presence of singularities in the boundary and/or initial conditions as well as those arising due to the geometry (the presence of obstructions in the flow) can lead to the generation of false extrema. A slope limiter can be applied to the DFEM solution in an attempt to remove false extrema from the solution of the transport equation and the utility of this approach is investigated.

Slab geometry investigations indicate that this has the potential to produce accurate solutions. The construction of multi-dimensional slope limiters for DFEM discretizations on unstructured meshes of finite elements with additional degrees of freedom e.g. quadrilaterals and hexahedra is being investigated. Initial results are presented for a simplistic slope limiter in order to demonstrate the technique.

2. SPATIAL DISCRETISATIONS

The steady-state transport equation can be written as follows,

$$\hat{\Omega} \cdot \nabla \psi(\underline{r}, \hat{\Omega}) + \sigma(\underline{r}) \psi(\underline{r}, \hat{\Omega}) = S(\underline{r}, \hat{\Omega}) \tag{1}$$

where ψ is the photon intensity, $\hat{\Omega}$ is the direction of particle propagation and $\underline{r}$ is the location in space, σ is the total cross-section for removal of photons from the beam (assumed to be isotropic) and S is a source term which includes contributions from both thermal emission and inscatter into the beam. The spatially discretized form of the equation is derived as follows.

A discontinuous finite element (DFEM) spatial discretization is constructed for the spatial variation of intensity and the source in each of the discrete propagation directions $\hat{\Omega}_m$ of the discrete ordinate method.

$$\psi(\underline{r}, \hat{\Omega}_m) = \sum_{i=1}^{n} \psi_{mi} \phi_i(\underline{r}) \tag{2}$$

and

$$S(\underline{r}, \hat{\Omega}_m) = \sum_{i=1}^{n} S_{mi} \phi_i(\underline{r}) \tag{3}$$

where $\phi_i(\underline{r})$ are the shape functions within the element obtained by an isoparametric transformation from the local element co-ordinates. The unknowns ψ_{mi}, S_{mi} are located at n specific locations within each cell (specifically for linear approximations the values are located at the vertices) and are unique to each element.

A weighted residual approach is used to derive the set of discrete equations. For each element the transport equation is multiplied by a set of weight functions $w_i(\underline{r})$ (one per unknown) and integrated over the cell volume. Two different choices of weight function are considered.

2.1 Galerkin weighting

Galerkin weighting corresponds to choosing the weight function to be the same as the finite element shape functions $w_i(\underline{r}) = \phi_i(\underline{r})$ and leads to the standard linear discontinuous finite element method. For isoparametric quadrilateral finite elements this method is referred to as the bi-linear discontinuous (BLD) method when applied to orthogonal meshes (Morel, 1993).

The streaming term is integrated by parts, converting the volume integral into a term involving the gradient of the weight function integrated over the element volume, together with an integral over the surface of the element,

$$\sum_{j=1}^{n} \left(-\hat{\Omega}_m \cdot \int \phi_j \nabla \phi_i dV + \int \sigma \phi_i \phi_j dV \right) \psi_{mj} + \hat{\Omega}_m \cdot \int_S \phi_i \psi \underline{dS} = \sum_{j=1}^{n} \left(\int \phi_i \phi_j dV \right) S_{mj} \tag{4}$$

The surface integral is evaluated using the values defined on the upwind side of each interface.

2.2 Petrov-Galerkin weighting

Petrov-Galerkin weighting which corresponds to the choice $w_i(\underline{r}) = \phi_i(\underline{r}) + \sigma^{-1}\hat{\Omega}_m \cdot \nabla\phi_i(\underline{r})$ which leads to the following discretization,

$$\sum_{j=1}^{n}\left(\int \sigma^{-1}(\hat{\Omega}_m\cdot\nabla\phi_j)(\hat{\Omega}_m\cdot\nabla\phi_i)dV + \int \sigma w_i\phi_j dV\right)\psi_{mj} + \hat{\Omega}_m\cdot\int_S \phi_i\psi\underline{dS} = \sum_{j=1}^{n}\left(\int\left(\phi_i + \sigma^{-1}\hat{\Omega}_m\cdot\nabla\phi_i\right)\phi_j dV\right)S_{mj} \quad (5)$$

In this case only the first term in the weight function has been integrated by parts to ensure that only first derivatives appear in this equation. The surface integral is identical to that for Galerkin weighting and is evaluated similarly.

This is equivalent to a Galerkin discretization of the scattering source iteration form of the self-adjoint angular flux (SAAF) second order transport equation (Morel, 1999),

$$-\hat{\Omega}\cdot\nabla(\sigma(\underline{r})^{-1}\hat{\Omega}\cdot\nabla\psi(\underline{r},\hat{\Omega})) + \sigma(\underline{r})\psi(\underline{r},\hat{\Omega}) = S(\underline{r},\hat{\Omega}) - \hat{\Omega}\cdot\nabla(\sigma(\underline{r})^{-1}S(\underline{r},\hat{\Omega})) \quad (6)$$

The upwind bias introduced into the weight function removes the instabilities associated with Galerkin weighting for non self-adjoint operators such as the the streaming operator. This allows robust solutions to be generated using CFEMs whilst also improving the positivity of the solution obtained by using discontinuous elements.

For the transport equation, the coefficient in the upwind term has been chosen to completely eliminate the streaming term in favour of the second order streamline diffusion term. Petrov-Galerkin weighting has also been applied to more general non-linear convection diffusion problems, leading to the stream-line upwind Petrov-Galerkin (SUPG) method (Brookes, 1982) used to solve the Euler equations using CFEMs.

2.3 Time dependence

Time dependent problems are solved by using backward Euler time differencing, which allows the time dependent equations to be converted into the same form as the steady-state equations, with suitably modified cross-sections. For the Galerkin weighted equations it is possible to use linear discontinuous finite elements (LDFEM) for the time variation (Wareing, 1999) in order to derive a scheme which is second order accurate in time; for Petrov-Galerkin weighting, this leads to the product of two delta functions and consequently only first order time differencing will be considered in this case.

2.4 Mass lumping

The DFEM discretizations of the transport equation considered in this paper do not produce strictly positive solutions. For thermal radiation problems positivity of the mean

intensity is important in order for the solution of the material energy equation to produce physically meaningful temperatures. In multi-dimensions the propagation directions are no longer aligned with the spatial mesh which leads to undershoots along the edges of the rays (although these are expected to be less pronounced for Petrov-Galerkin weighting).

An additional difficulty for thermal radiation problems is that it is not possible to resolve spatial scales down to a mean free path in typical problems, so the differencing scheme needs to be robust for large optical depth cells. Once the optical depth (τ) exceeds a certain number of mean free paths linear elements are unable to accurately resolve the gradient within the cell and it is no longer possible to maintain the positivity for the outgoing intensities. A slab geometry analysis for a steady-state pure absorber indicates that this occurs for $\tau > 3$ for Galerkin weighting and $\tau^2 > 6$ for Petrov-Galerkin weighting.

The simplest approach to overcoming these deficiencies is to mass lump the removal operator in the discrete equations (Morel, 1992), together with the corresponding source term on the right hand side of the transport equation for consistency. As the results in this paper will show, lumping has the desired effect but at the cost of significantly degrading the accuracy of transient solutions by smearing the profile of the ray and perturbing the propagation direction.

Mass lumped solutions using Petrov-Galerkin weighting are significantly more accurate in terms of the amount of attenuation for opaque cells compared with Galerkin weighting, although neither solution is very accurate beyond a few mean free paths. This becomes less important once the radiation field equilibrates with the material, absorption and re-emission driving the propagation of the radiation front rather than direct transmission through the medium.

An alternative strategy is proposed based on the use of slope limiters to suppress the growth of unphysical extrema in the hope that this will be sufficient to provide robustness while maintaining the accuracy of the radiation transport solution. Restricting mass lumping to opaque cells may be the best compromise that can be achieved between robustness in these regions and accuracy in transparent parts of the problem.

2.5 Diffusion limit behaviour

Both schemes correspond to accurate CFEM discretizations of the radiation diffusion equation in the interior of diffuse regions, with an approximate Eddington tensor whose accuracy depends on the choice of the discrete ordinate quadrature set. For the Petrov-Galerkin discretization the diffusion limit analysis is trivial, while an analysis of the Galerkin weighted scheme indicates that with mass lumping this corresponds to a discretization of the diffusion equation with the gradient term averaged over the cell (Smedley-Stevenson, 2000[a]).

At the boundary between transparent and unresolved optically thick diffuse regions, the amount of radiation penetrating the diffuse region is sensitive to the spatial discretization. For the Galerkin discretization, the solution in the interior of unresolved diffuse re-

gions is remarkably accurate irrespective of the angle of incidence, the error being limited to the first cell within the region.

The Petrov-Galerkin discretization exhibits similar behaviour to the CFEM solution of the even parity equation (Adams, 1991). Large errors are present in the amount of radiation penetrating the region for radiation which is obliquely or normally incident. This deficiency is still present for the SAAF second order transport equation for both continuous and discontinuous finite element discretizations.

3. SLOPE LIMITERS

The construction and application of slope limiters has been studied largely in the context of piecewise constant approximations on regular orthogonal mesh. Some work has also been performed for discontinuous finite elements in determining slope limiters which bound the total variation (TV) of the solution as part of the Runge-Kutta discontinuous Galerkin (RKDG) method for non-linear convection problems (Cockburn, 1999).

In multi-dimensions, the slope limiters constructed for the RKDG method are based on the use of linear finite elements on orthogonal meshes, where the unknowns are the mean value and gradients up to the order of the required approximation. For meshes composed of triangles or hexahedra, the unknowns are located along the sides of the elements and in either case the finite element shape functions are chosen to be mutually orthogonal.

The construction of slope limiters in slab geometry is a relatively simple process as there are no additional degrees of freedom within the elements. The same limiter can be applied irrespective of whether the unknowns are taken to be centered at specific locations in the element or a set of mutually orthogonal finite element basis function are used.

3.1 Slab geometry slope limiter

The TVBM (total variation bounded in the means) generalization of the slope limiter $\Lambda\Pi_h^1$ from the RKDG method is studied in this paper. This is based on a less restrictive form of the slope limiter from the MUSCL scheme of Van Leer, with a modified *minmod* function which allows for a bounded amount of curvature in the solution (Cockburn, 1999). Numerical experimentation has shown that of all the slab geometry limiters described in this reference, this produces superior results.

The values of the function u obtained by applying the $\Lambda\Pi_h^1$ slope limiter to the discontinuous piecewise linear function v are given by

$$u^-_{j+1/2} = \overline{v}_j + \overline{m}(v^-_{j+1/2} - \overline{v}_j, \overline{v}_j - \overline{v}_{j-1}, \overline{v}_{j+1} - \overline{v}_j) \tag{7}$$

$$u^+_{j-1/2} = \overline{v}_j - \overline{m}(\overline{v}_j - v^+_{j-1/2}, \overline{v}_j - \overline{v}_{j-1}, \overline{v}_{j+1} - \overline{v}_j) \tag{8}$$

where $\overline{v}$ are the cell averaged values and $v^+_{j-1/2}$ and $v^-_{j+1/2}$ are the values at the left and right edges of cell j. This is valid for uniform mesh spacings but is easily generalized to

the case of non-uniform meshes.

The *minmod* function m is defined as follows:

$$m(a_1,\cdots,a_m) = \begin{cases} s\min_{1\le n\le m}|a_n| & \text{if } s = sign(a_1) = \cdots = sign(a_m), \\ 0 & \text{otherwise} \end{cases} \tag{9}$$

and the total variation bounded (TVB) corrected *minmod* function $\overline{m}$ is defined as follows:

$$\overline{m}(a_1,\cdots,a_m) = \begin{cases} a_1 & \text{if } |a_1| \le M(\Delta x)^2, \\ m(a_1,\cdots,a_m) & \text{otherwise} \end{cases} \tag{10}$$

where M is a given constant which is an upper bound on the absolute value of the second derivative of the solution at local extrema, estimated from the initial conditions. This modification is important for the advection of the Gaussian profile as it prevents erosion of the peak value by disabling the limiter for smooth extrema.

Alternative procedures have also been investigated by the author including the inclusion of an artificial diffusion term, with the amount of dissipation chosen so that the total variation of the solution does not increase. This produces excess dissipation relative to the use of the slope limiter described above and is not considered further.

3.2 Multi-dimensional slope limiters

In multi-dimensions, the generalization of the slope limiter derived for the RKDG method to the isoparametric finite elements from the Lagrangian mesh is not straightforward, due to the extra degrees of freedom that these elements have in terms of the variation of the solution within each element.

A modified slope is determined by limiting the cell averaged gradient with respect to the local values of the gradient obtained from the mean values in surrounding elements. In two dimensions a unique bi-linear function can be constructed from the cell averaged value and two mean values defined in cells on adjacent sides, the mean values being assumed to be located at the centroid of each element (and similarly in three dimensions based on three cells across adjacent faces).

An average is taken of all the gradients which can be defined as above. This serves to define the orientation of the modified slope. The magnitude is determined by a generalization of the scheme used in slab geometry. The cell averaged gradient and each of the individual gradients are dotted into this direction. The magnitude of the modified gradient is defined by the applying the *minmod* function to these values.

As in the slab geometry case, it is possible to allow greater flexibility by using the TVB corrected *minmod* function $\overline{m}$. The gradient constructed in this manner provides greater flexibility with extrema being allowed to develop while constraining the amount of curvature in the resulting solution. The results presented in this paper are based on the standard *minmod* function obtained by setting $M = 0$, as the initial solution is set equal to zero for the ray propagation tests.

The nodal values within the element are reconstructed based on the mean value and the modified slope. For linear finite elements the nodes are chosen so that the cross-derivative terms (u_{xy}, u_{xz} and u_{yz}) vanish when integrated over the each cell. This leads to a system of four linear equations in each quadrilateral element, solved directly by Gaussian elimination. The curvature of the solution within the element is removed, suppressing the extra degrees of freedom, irrespective of whether the slope is changed. Diffusion terms within each element are suppressed in the DFEM discretization and if this proves to be undesirable an alternative strategy should be developed.

4. WAVE PROPAGATION TESTS

The propagation of wave profiles is studied in slab geometry, in order to gain an insight into the systematic behaviour of the relationship between the spatial and temporal differencing schemes. For propagation through vacuum in slab geometry the solutions with Galerkin and Petrov-Galerkin weighting are similar (the latter is dominated by the explicit streaming term on the right-hand side of the equation) and for conciseness the Petrov-Galerkin solutions are not reproduced in this section.

A fixed timestep $cdt = 0.1$ is used to advect Gaussian and step profiles 20 cells to the right (the cell width $dx = 1$ and the direction cosine $\mu = 1$). Figure 1 shows that the results for the Gaussian profile, which is significantly diffused for backward Euler time differencing. Time resolved solutions can be obtained by using the LDFEM timestepping scheme or cutting the timestep by roughly an order of magnitude. These are unaffected by the modified slope limiter described in section 3.1. For the step profile shown in figure 2 significant under and overshoots develop as the time dependent behaviour is resolved. Applying the slope limiter to the results suppresses the growth of these extrema.

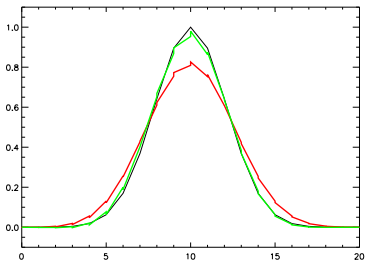

Fig. 1: LDFEM (green) versus backward Euler differencing (red) for the advection of a Gaussian profile.

At this point it is worth making a few general observations about the solutions obtained for absorbing media. Fundamentally, the inclusion of absorption in the equations does not lead to any additional difficulties. However, the timestep needs to be restricted for both forms of the transport equation as the opacity of the cells is increased (irrespective of the order of the temporal differencing). The error in the total amount of attenuation depends on the timestep and the cross-section.

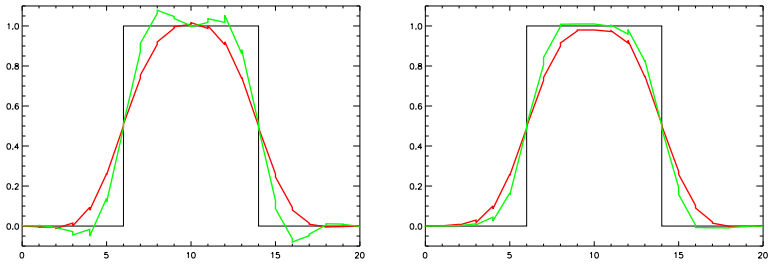

Fig. 2 As figure 1 for a step profile, with the slope limiter applied (right).

The use of large timesteps in the Galerkin weighted DFEM equations leads to an unphysical reduction in the propagation velocity of the profile as the amount of attenuation increases. For Petrov-Galerkin weighting unphysical gradients develop within each cell for the step profile, although the phase velocity is unaffected.

This section concludes by illustrating the effect of mass lumping the removal operator on the advection of the Gaussian and step profiles (see figure 3). The numerical diffusion introduced by lumping retards the propagation velocity, leading to the development of a distinct front to back asymmetry in the solutions.

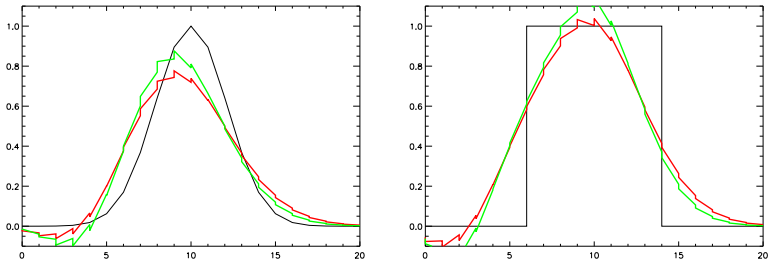

Fig. 3 Solutions obtained by lumping the removal operator.

4.1 2D ray propagation

Mathews (1999) compares the results for ray propagation in 2D planar geometry through a strongly attenuating medium, for a variety of discretizations of the first order transport equation including DFEM and characteristics based approaches. Significantly, his results show that the diamond difference approximation without the negative flux fixup procedure leads to lateral oscillations which are undamped relative to the intended ray.

His studies of DFEM methods are restricted to considering the unlumped Galerkin weighted DFEM discretization of the first order transport equation for orthogonal meshes, using linear discontinuous (LD) and bi-linear discontinuous (BLD) finite elements. The LD results show a large but rapidly damped oscillation to the left of the ray, while the BLD method leads to better ray quality with a small negative trough on either side but no sign

of oscillations. For both methods the ray propagates in almost the right direction and the amount of attenuation as the ray exits the mesh is in error by only 6%.

In this paper additional DFEM results are obtained based on Petrov-Galerkin weighting and the effect of mass lumping the removal operator (in order to improve the positivity of the solution) is demonstrated. In addition to the steady-state behaviour, the time-dependent propagation of the ray is considered. The smoothing of the singularity in the boundary conditions over space is equivalent to smearing out the arrival of the signal over time for time dependent problems and this has important implications for the accuracy of the scheme when comparing with benchmark solutions.

The problem consists of propagating a ray through a purely absorbing medium (a square 25 units wide) with cross-section $\sigma = 1$ which is modeled using a 50×50 mesh of square cells. The direction of ray is taken from the level-symmetric S_4 quadrature set and has direction cosines $\Omega_x = 0.35000212$ and $\Omega_y = 0.8688903$. It enters through the bottom boundary of the cell closest to the origin.

The various DFEM schemes are abbreviated as follows: G corresponds to the Galerkin weight scheme while PG corresponds to Petrov-Galerkin weighting, SL indicates that the slope limiter described in section 3.2 has been applied to the DFEM solution at the end of each timestep (the steady-state results are obtained from the time-dependent coding) and L indicates that mass lumping has been invoked for the removal operator.

The application of a slope limiter to modify the gradients of the DFEM solution has similarities with the non-linear fixes applied to ensure stability and/or positivity for other discretizations of the transport equation. In these methods a non-linear correction is applied to the solution within the cell based on upwind information. By contrast, the slope limiter approach makes use of information about the solution in neighbouring cells in both the upwind and downwind directions to limit the gradients in the DFEM solution.

Figure 4 compares steady-state results for the ray propagation. These graphs show the value of the flux along the top edge of the cells, normalized relative to the exact amount of attenuation from row to row. The orientation of the plots is chosen so that the ray direction corresponds to the vertical axis. Galerkin and Petrov-Galerkin weighting both produce a sharp ray, with undershoots to either side. The Galerkin results are more accurate both in terms of the propagation direction and the overall amount of attenuation.

The application of the slope limiter significantly reduces the magnitude of the undershoots without significantly perturbing the ray direction. The amount of smoothing of the peak of the ray can be controlled by varying the details of the limiter. For the slope limiter described in this paper the curvature of the solution within each element is suppressed. The Petrov-Galerkin formulation reduces to a variant of the Galerkin discretization, consequently for a time resolved solution the two sets of results are indistinguishable.

The effect of mass lumping is both to smear the ray out over space and perturb the ray direction, while significantly under predicting the amount of attenuation. The smearing of the ray is more pronounced with Petrov-Galerkin weighting. The error in the number of particles leaving the mesh is presented in table 1. The ray travels 28.77 mean free paths

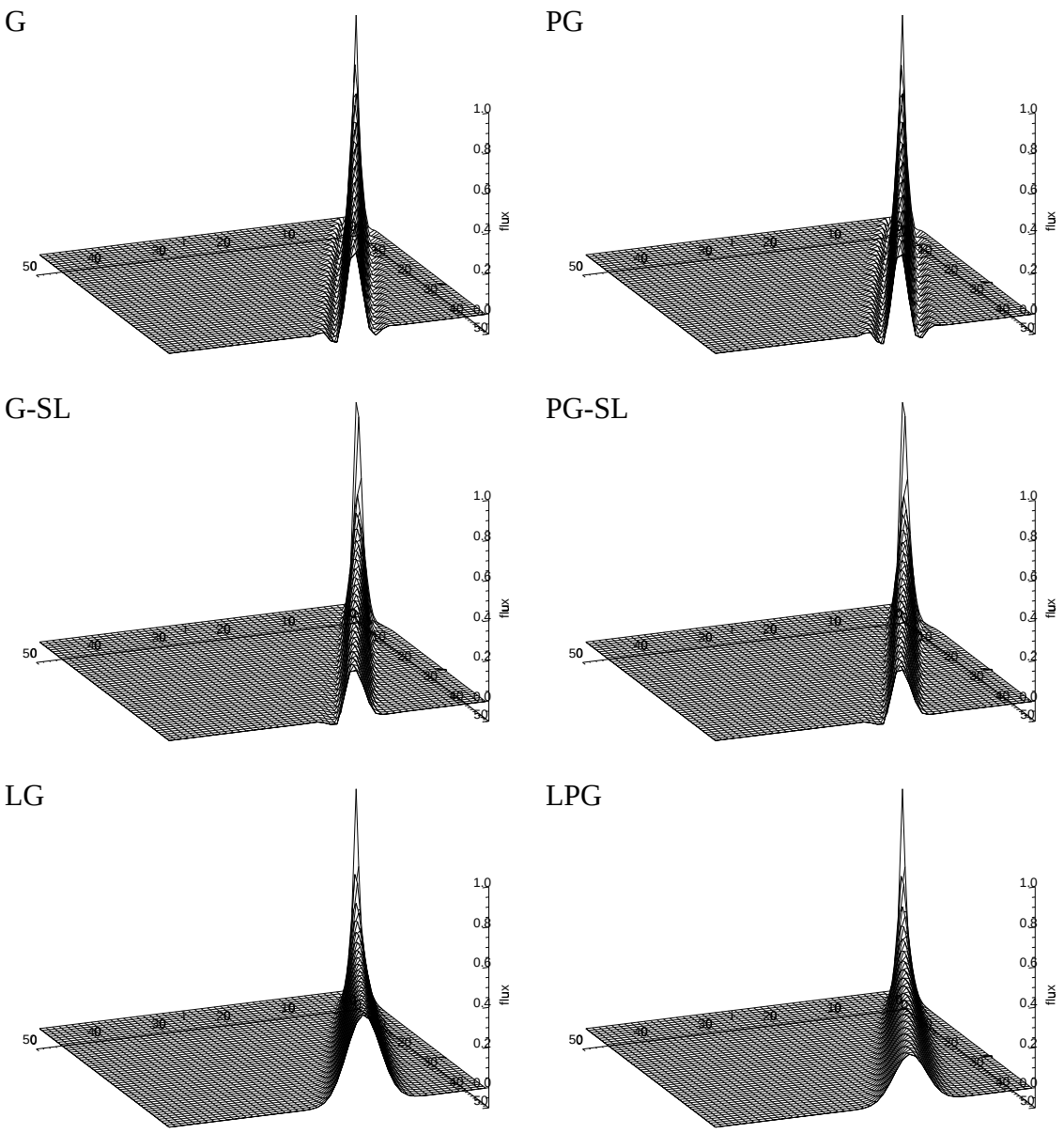

Fig. 4 Steady state solution of the attenuating ray propagation problem

across the mesh, so even with mass lumping the attenuation is reasonably well predicted.

Table 1 Particles flux out of the top of the mesh relative to the exact value.

scheme	%age of exact value	scheme	%age of exact value
G	93.5	PG	83.5
G-SL	74.5	PG-SL	74
LG	285	LPG	153

Investigating the details of the solution it is clear that the slope limiter has the effect of degrading the amount of attenuation close to the source by reducing the accuracy of the gradients as calculated by the DFEM method. The overall accuracy is still reasonable but locally the accuracy of the solution can be degraded.

The benefit of applying the slope limiter is more clearly seen by studying the transient propagation behaviour. It is easier to visualize the results by rotating the plots so that the ray direction lies in the plane of the page. Figures 5 and 6 show the ray after it has propagated 20 and 40 cell widths respectively. The solutions are calculated using backward Euler time differencing with an adaptive time stepping scheme which attempts to control the error in the solution.

Significant oscillations develop ahead of the wavefront when solving the unlumped equations. This is a consequence of the backward Euler differencing. The cross section is replaced by a $\sigma + 1/(cdt)$ where cdt is the distance the signal can propagate during the current timestep. The physical interpretation is that the position of the wavefront is updated by exponentially attenuating the solution over this distance in an attempt to obtain the correct propagation velocity. For small timesteps, the linear approximation of the gradient leads to undershoots (similar to those that develop for large optical depth cells) and the front of the wave is characterized by these oscillations.

The mass lumped solutions smear the wavefront significantly over space in an attempt to maintain the positivity of the solution by using a strictly positive but less accurate approximation for the exponential decay. Due to underestimating the amount of attenuation, mass lumping allows a significant fraction of the signal to propagate distances greater than cdt. With the slope limiter the wavefront is significantly steeper and very few particles are allowed to propagate ahead of the correct position of the wave.

5. CONCLUSIONS

Slab geometry results for the advection of various profiles indicate that the Galerkin DFEM discretization of the time dependent transport equation produces accurate answers for smooth profiles, but if there are discontinuities in the initial profile (or from the boundary conditions) these lead to the creation of new extrema in the DFEM solution. It is possible to suppress the growth of these extrema by applying a slope limiter to the finite element solution at the end of each timestep.

G

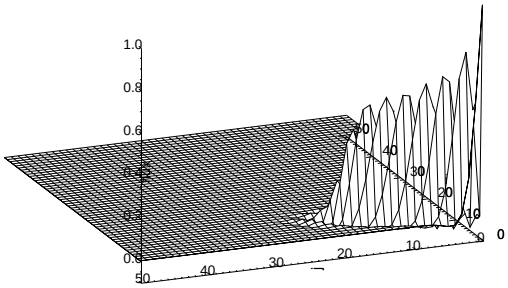

PG

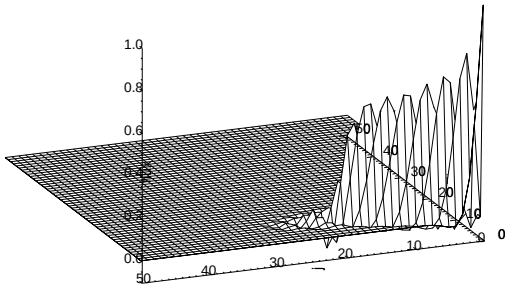

G-SL

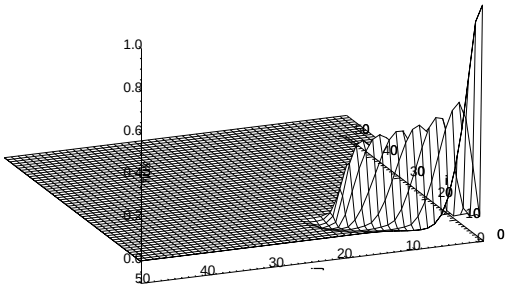

PG-SL

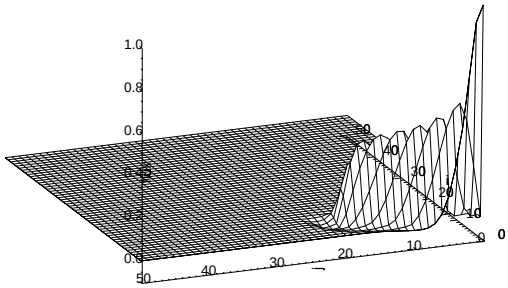

LG

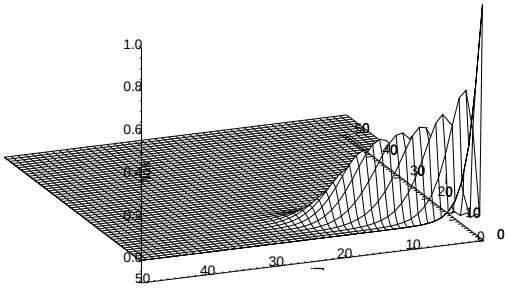

LPG

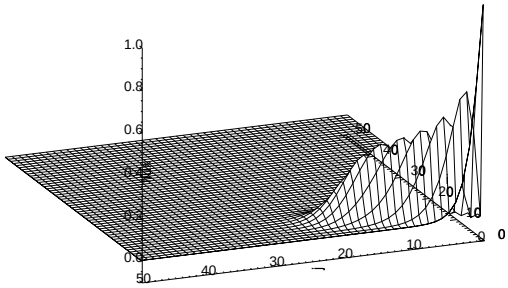

Fig. 5 Solution of the attenuating ray propagation problem for $ct = 10$

G

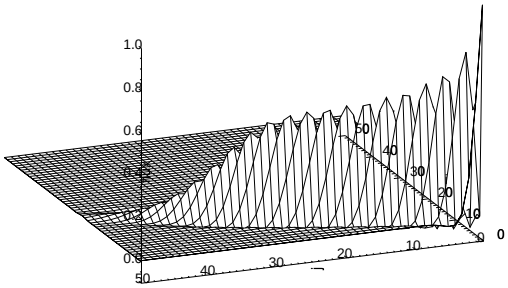

PG

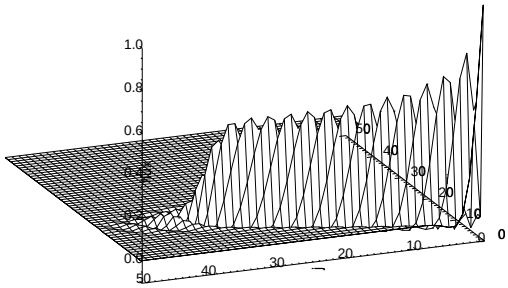

G-SL

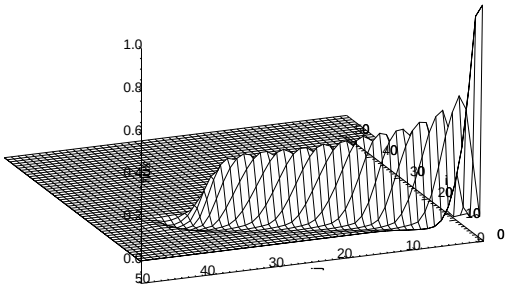

PG-SL

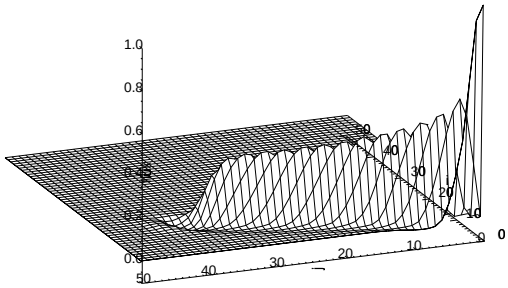

LG

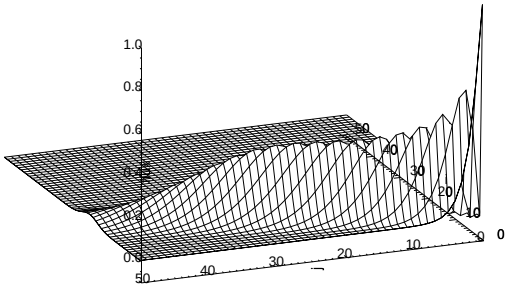

LPG

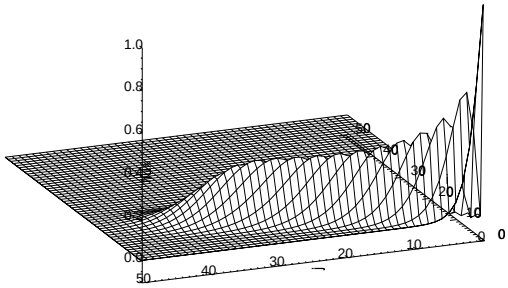

Fig. 6 Solution of the attenuating ray propagation problem for $ct = 20$

The DFEM discretization of the streaming operator leads to undershoots on either side of the ray in two-dimensions. Compared with Galerkin weighting, Petrov-Galerkin weighting is not as accurate in terms of the total amount of attenuation but for transient problems it leads to an improved wavefront profile. Slope limiting is effective at suppressing both the undershoots on either side of the ray and oscillations at the head of the wavefront for transient problems. More sophisticated slope limiters are desirable for general unstructured meshes and this is left as a topic for future research.

The effect of mass lumping is to improve the positivity of the solution at the expense of significantly degrading the accuracy of the transport solution. In multi-dimensions this leads to significant smearing of the ray profile and produces large errors in the amount of attenuation and the location of the wavefront in transient problems. Consequently, mass lumping should not be invoked unless it is essential for robustness.

It could be argued that the problems considered in this paper all contain strong singularities and therefore emphasize a worst case scenario. These types of singularities are not uncommon in general transport problems and it is desirable for the solution algorithm to perform reasonably well for even the most difficult cases. It is possible for these undesirable features to be present in the angular flux while still producing an apparently reasonable scalar flux distribution.

6. ACKNOWLEDGEMENTS

The author would like to acknowledge the assistance of Andrew Barlow in the Computational Physics group at AWE for providing help and advice on the construction of multi-dimensional slope limiters. I would also like to thank Chris Pain in the Computational Physics and Geophysics department at Imperial College for sharing his ideas on possible mechanisms for improving the fidelity of DFEM solutions of the transport equation.

7. REFERENCES

Adams, M.L., 1991. Even-parity finite-element transport methods in the diffusion limit. *Prog. in Nucl. Energy*, **25**, 159–198.

Cockburn, B., 1999. Discontinuous Galerkin Methods for Convection-Dominated Problems. In: Barth, T.J., Deconinck, H. (Eds.), *High-Order Methods for Computational Physics*, Springer, pp. 69–224.

Brooks, A.N., and Hughes, T.J.R., 1982. Streamline Upwind/Petrov-Galerkin Formulations for Convection Dominated Flows with Particular Emphasis on the Incompressible Navier-Stokes Equations. Comput. Meths. in Appl. Mechs. and Eng., **32**, 199–259.

Mathews, K.A., 1999. On the Propagation of Rays in Discrete Ordinates. *Nucl. Sci. Eng.*, **132**, 155–180.

Morel, J.E., Dendy, Jr., J.E., and Wareing, T.A., 1993. Diffusion-Accelerated Solution of the Two-Dimensional S_n Equations with Bilinear-Discontinuous Differencing. *Nucl. Sci. Eng.*, **115**, 304.

Morel, J.E., Wareing, T.A., and Smith, K., 1996. A Linear-Discontinuous Spatial Differencing Scheme for S_n Radiative Transfer Calculations. *JCP*, **128**, 445–462.

Morel, J.E., and McGhee, J.M., 1999. A Self-Adjoint Angular Flux Equation. *Nucl. Sci. Eng.*, **132**, 312–325.

Smedley-Stevenson, R.P. Studies of Deterministic Transport Methods for Thermal Radiation on Unstructured Meshes. In Proc. Int. Topl. Mtg on Advances in Reactor Physics and Mathematics and Computation into the Next Millennium, Pittsburgh, PA, USA, 7-12 May 2000.

Smedley-Stevenson, R.P., 2000[a]. Thermal Radiation Transport on Unstructured Finite Element Meshes. *Trans. ANS*, **83**, 243–246.

Su, B., and Olson, G.L., 1997. An Analytical Benchmark for Non-Equilibrium Radiative Transfer in an Isotropically Scattering Medium *Ann. Nucl. Energy*, **24**, 1035.

Wareing, T.A., Morel, J.E., and McGhee, J.M. A Diffusion Synthetic Acceleration Method for the S_N Equations With Discontinuous Finite Element Space and Time Differencing. In Proc. Int. Topl. Mtg on Mathematics and Computation, Reactor Physics and Environmental Analysis in Nuclear Applications, Madrid, Spain, September 1999.